American Mineralogist, Volume 92, pages 267–280, 2007

Significance of aluminum phosphate-sulfate minerals associated with U unconformity-type deposits: The Athabasca basin, Canada

Stéphane Gaboreau,[1,2,*] Michel Cuney,[3] Dave Quirt,[4] Daniel Beaufort,[1] Patricia Patrier,[1] and Régis Mathieu[5]

[1]Laboratoire HydrASA CNRS-UMR 6532, Université de Poitiers, bât de Géologie, 40 Avenue du Recteur Pineau, 86022 Poitiers-Cedex, France
[2]ERM SARL, Laboratoire-Bureaux, Université de Poitiers, bât de Géologie, 40 Avenue du Recteur Pineau, 86022 Poitiers-Cedex, France
[3]CREGU UMR G2R 7566, Université Henri Poincaré, Nancy I, BP 23-F54 506 Vandoeuvre les Nancy cedex, France
[4]COGEMA Resources Inc., P.O. Box 9204, Saskatoon, SK S7K 3X5, Canada
[5]COGEMA-BUM-DEX, 2 rue Paul Dautier, BP 4, F 78141 Vélizy Cedex, France

Abstract

Aluminum phosphate-sulfate (APS) minerals formed around the Athabasca unconformity-type deposits and those from their Australian counterparts are chemically very similar showing the same continuum between the diagenetic Sr-rich APS minerals of the barren sandstones and the LREE-rich composition of the APS minerals in the hydrothermally altered sandstone. The P- and LREE-rich compositions were controlled by the transport and the redistribution of P and LREE elements released from the dissolution of phosphate minerals (principally monazite) in the basement rocks and in the basin during the syn-ore alteration processes.

The S/Sr ratio measured in the APS minerals from unaltered sandstone away from the unconformity and any mineralization is preserved during the syn-ore alteration processes suggesting that the fluids involved in both the deep burial diagenetic processes and the syn-ore alteration system were derived from a similar diagenetic reservoir in both the Athabasca and Kombolgie regions.

The trioctahedral chlorite host-rock alteration around the Australian basement-hosted U deposits, as compared to the illite and sudoite associated with the Athabasca basement-hosted, along with the more LREE-rich APS compositions in the Australian deposits, suggests that the pH and oxygen fugacity (f_{O_2}) of the syn-ore fluids differed in the alteration systems of the two regions at the time of the U deposition.

Keywords: APS minerals, florencite, goyazite, svanbergite, unconformity-type uranium deposits, Athabasca basin, clay minerals, geochemistry

Introduction

Aluminum phosphate-sulfate (APS) minerals occur in a wide range of geological environments, ranging from surficial weathering through sedimentary, diagenetic, hydrothermal, and metamorphic environments, to post-magmatic systems (Dill 2001). These minerals belong to the alunite supergroup (Scott 1987; Jambor 1999) and crystallize most commonly as authigenic pseudocubic (rhombohedral) crystals.

APS minerals have been described from various middle Proterozoic sandstone basins, including the Athabasca (Hoeve and Quirt 1984; Wilson 1985; Quirt et al. 1991; Mwenifumbo et al. 2002; Lorilleux et al. 2003) and Thelon (Miller 1983) Basins in Canada and the Kombolgie Formation of the McArthur basin in Australia (Beaufort et al. 2005; Gaboreau et al. 2005), as well as from Cretaceous sandstone in Nova Scotia, Canada (Pe-Piper and Dolansky 2005). However, generally APS minerals have been neglected by geologists and geochemists because of the minute size of the crystals (<0.1–10 μm) and their low concentration (generally less than 0.05 wt%), which have hindered their identification by conventional microscopic techniques. In addition, their very low solubility at low temperatures renders them inert to sequential extraction in solvents.

In particular, APS minerals are abundant in the clay mineral host-rock alteration assemblages associated with some uranium fields in these middle Proterozoic basins (Miller 1983; Hoeve and Quirt 1984; Wilson 1985; Quirt et al. 1991; Fayek and Kyser 1997; Lorilleux 2001; Beaufort et al. 2005; Gaboreau et al. 2005). The uranium fields in Canada and Australia contain large-tonnage unconformity-type uranium deposits and several important prospects (Sibbald et al. 1990; Andrade et al. 2002). Few systematic investigations have been performed on the APS minerals in these deposits (e.g., Gaboreau et al. 2005) and little data are available on the APS compositional variations in relation to the uranium deposits (e.g., Quirt et al. 1991; Gaboreau et al. 2005). However, it is documented that the formation of these deposits was controlled by physicochemical conditions (Eh, pH, constituent element activities, *P*, *T*), to which the APS minerals are particularly sensitive (Dill 2001; Kolitsch and Pring 2001).

The aim of this study is to clarify the nature and the origin of the APS minerals present in the middle Proterozoic Athabasca sandstone and in the host-rock alteration halos that envelops the Athabasca unconformity-type uranium ore bodies. Spatial variations of both crystal chemistry and phase relationships

* E-mail: stephane.gaboreau@ext.univ-poitiers.fr

with clay minerals, on a regional scale, have been investigated to improve our knowledge on the suitability of these minerals to indicate the paleoconditions at which the alteration processes relative to the uranium deposition operated. These results are compared with those already obtained for the alteration halos associated with the unconformity-type uranium deposits of the Australian counterpart (Gaboreau et al. 2005) to confirm the utility of these minerals as a mineralogical tool for worldwide exploration of unconformity-related high-grade uranium orebodies.

Regional geological setting

The Mesoproterozoic Athabasca Basin (Fig. 1) occupies nearly one-third of the surface area of the exposed Canadian Shield of northern Saskatchewan and extends to the west into northern Alberta. The basin presently extends about 350 km east to west and 200 km north to south, with a maximum thickness of 1500 m at Rumple Lake (Fig. 1). However, the initial size of the basin was much larger as attested by Athabasca sandstone outcrops located away from the current basin margin, such as the Reilly Basin located about 80 km to the southeast of the eastern margin of the Athabasca Basin (Ramaekers and Catuneanu 2004), and much thicker (5 to 6 km) according to estimations derived from fluid inclusion studies (Pagel et al. 1980; Derome et al. 2002, 2005). The basin contains the preserved portion of the unmetamorphosed, generally undeformed, PaleoHelikian Athabasca Group that is dominantly composed of variable hematitic, coarse fluvial quartz sandstones and conglomerates, and it hosts numerous high-grade unconformity-type uranium deposits.

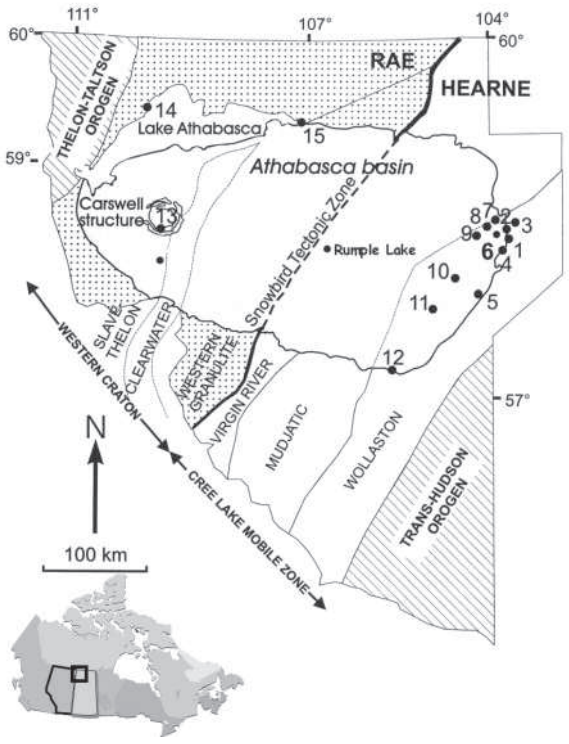

Figure 1. Crustal domains and lithostructural provinces of the sub-Athabasca basement, studied areas and main unconformity-type deposits in the Athabasca Basin (modified from Ruzicka 1993). RAE = Rae lithostructural province, HEARNE = Hearne lithostructural province. 1 = Rabbit Lake, 2 = Collins Bay, 3 = Eagle Point, 4 = Raven, 5 = West Bear, 6 = Horseshoe, 7 = McClean Lake, 8 = Dawn Lake, 9 = Midwest, 10 = Cigar Lake, 11 = McArthur River, 12 = Key Lake, 13 = Cluff Lake, 14 = Maurice Bay, 15 = Fond du Lac.

The Athabasca Group comprises four major fining-upward orthoquartzitic clastic sequences composed of variably hematitic, coarse fluvial quartz sandstones and conglomerates, with minor silty marine to lacustrine clastic sedimentary intervals and finally capped by shale and dolomite, deposited during the PaleoHelikian ~1750–1650 Ma (Ramaekers et al. 2001; Rainbird et al. 2005). The sediments are interpreted to have been deposited in major river systems and near shore to shallow-shelf environments in a tectonically active sedimentary basin (Ramaekers et al. 2001, 2005).

The basin is an intracratonic successor ("second generation") basin developed in response to continued uplifts and plate movement after the initial Trans-Hudson Orogeny (THO). Its age relationship to the 1860–1775 Ma Trans-Hudson Orogeny (Annesley et al. 2005) shows that it is not the primary foreland sequence (Ramaekers et al. 2005).

The Athabasca Group can be subdivided into several fining-upward sequences that are separated by unconformities or by coarse-grained units that abruptly overlie finer grained units of the previous sequence. The overall fine-grained, gritty red-bed sedimentary rocks unconformably overlie a crystalline basement and consist of conglomerate, sandstone, pebbly sandstone, and minor siltstones of the Fair Point, Manitou Falls, Lazenby Lake, Wolverine Point, Locker Lake, and Otherside formations, followed by the silstone/mudstones and dolstones of the Douglas and Carswell formations, respectively (Ramaekers 1981, 1990; Ramaekers et al. 2001, 2005). The lithostratigraphic subdivisions are based upon changes in the size and/or abundance of granules, pebbles, clay intraclasts, conglomerates, and mudstones. The Athabasca Group is generally flat-lying and undeformed except within the Carswell structure, where bedding is steeply dipping and locally overturned. The sandstone is unmetamorphosed but matrix minerals were extensively recrystallized during prolonged diagenesis at temperatures of 150–200 °C (Hoeve and Quirt 1984; Kotzer and Kyser 1995; Derome et al. 2005). A well-developed regolithic profile on the amphibolite- to granulite-grade crystalline metamorphic basement rocks underlying the Athabasca Group extends to a depth of several meters to several tens of meters according to the type of lithology and the importance of the tectonic structures (Macdonald 1980, 1985).

The Paleoproterozoic and Archean sub-Athabasca rocks are subdivided into two major tectonic elements, the Rae Province in the west and the Hearne Province in the east, which were affected to varying degrees by the TransHudson Orogeny (1860–1775 Ma) and the Thelon-Talston Orogeny (~2000–1900 Ma) in the western and eastern Athabasca, respectively (Fig. 1). These two elements are bounded by major structural breaks, such as the Snowbird Tectonic Zone (STZ), and are further subdivided into smaller lithostructural domains. In the eastern Athabasca region, the Paleoproterozoic metasedimentary rocks are members of the Wollaston Domain (Lewry and Sibbald 1979, 1980; Macdonald 1985; Annesley et al. 2005) and

have been intruded by Hudsonian granitoid rocks. Pelitic to psammitic gneisses, commonly with anatectic leucosomes, unconformably overlie the Archean granitoid gneisses and typically consist of quartz, plagioclase, biotite, cordierite, garnet, sillimanite, and tourmaline (Ey et al. 1991; Marlatt et al. 1992; Annesley et al. 2005). The pelitic and psammopelitic gneisses are locally graphitic. Metaquartzite units occur locally, grade into psammitic gneisses, and are generally separated by intervals of garnet-cordierite pelitic gneiss (Marlatt et al. 1992). In the western Athabasca region, the Taltson domain, the extent of which has been recently extended under much of the western part of the Athabasca Basin (Brouand et al. 2003; Card et al. 2003, 2006), includes packages of graphitic aluminous metasedimentary lithologies, including garnetite, intercalated between felsic orthogneiss units (Card 2001, 2002).

The world-class, high-grade, unconformity-type uranium deposits associated with the Athabasca Basin represent the most significant high-grade, low-cost uranium resource currently being exploited on a worldwide basis and has an estimated resource in excess of 375 000 t U (1371 M lbs. U_3O_8). These epigenetic deposits formed through the circulation of saline diagenetic brines in the middle Proterozoic Athabasca sedimentary basin, and the redox interaction of these oxidized basinal brines with reduced basement fluids (Hoeve and Sibbald 1978; Hoeve and Quirt 1984; Kotzer and Kyser 1995). The circulation within the sandstone and basement of reactive, oxidized, highly saline, Ca-Na-Mg brines, generated at the base of the thick, organic matter-free and K-feldspar-free Athabasca sandstone basin, resulted in scavenging of uranium even from refractory minerals, such as monazite. The nature of the uranium precipitation mechanism is, however, still not well constrained (Cuney 2005; Derome et al. 2005), although a reduction process is generally accepted. The uranium ore occurs close to the unconformity separating the Athabasca Group sediments and the underlying Archean-Paleoproterozoic crystalline basement rocks, but some occurs down to 450 m into the basement, as in the Eagle Point deposit (deposit 3 in Fig. 1). The ore zones are spatially controlled by faults crosscutting this unconformity and rooted in graphite-rich metamorphic rocks.

The formation of mineralization-related, clay-rich, host-rock alteration halos was associated with the fluid interactions and these halos envelop the main ore-controlling structures (Hoeve and Sibbald 1978; Hoeve and Quirt 1984; Pacquet and Weber 1993; Percival et al. 1993; McGill et al. 1993; Kotzer and Kyser 1995; Thomas et al. 2000; Lorilleux et al. 2002, 2003; Kister et al. 2005). These alteration halos overprinted the original sandstone and basement mineral parageneses and thus the alteration minerals record the ancient mineralizing fluid flow pathways and form a major exploration guide to the location of uranium mineralization (Hoeve and Quirt 1984; Kister et al. 2005). Due to their very high grade and reserve potential, unconformity-type uranium deposits have become the most sought-after uranium targets over the last 20 years and will continue to be the deposit of choice in the near future (Thomas et al. 2002).

Numerous metallogenetic investigations have been performed on the unconformity-type deposits over the last several decades, including Hoeve and Quirt (1984), Ruzicka (1993), Kotzer and Kyser (1995), Fayek and Kyser (1997), Quirt (1997b, 2001, 2003), Hecht and Cuney (2000), Lorilleux et al. (2002, 2003), Gaboreau et al. (2003), Ramaekers et al. (2005), Kister et al. (2005), Laverret et al. (2005), and Derome et al. (2005). However, investigations on the APS present in the regional sandstone and in the alteration halos have been few and of varying detail (Quirt et al. 1991; Gaboreau et al. 2005).

Sampling

All of the rock samples were taken from drill core, which were used to prepare standard polished thin sections. More than 300 samples, representing 15 drill holes, covering the eastern and western parts of the Athabasca basin, were studied, including the Rumple Lake stratigraphic drill hole situated in the middle of the basin.

Samples (Table 1, Fig. 1) include representative material taken from throughout the sandstone column and the basement lithologies. The samples were selected according to distance from ore deposits, discontinuities (fault, brecciated zones, unconformity), and types of clay alteration. From these criteria, three major groups of samples were distinguished: (1) barren samples from regional drill holes, such as Erica 1 and Rumple Lake; (2) "anomalous" samples from in or near uranium anomalies on either side of the unconformity; and (3) samples from the vicinity of the major uranium deposits in the Athabasca basin, including Cigar Lake, McArthur River, and Shea Creek (Anne area).

Methods

Samples were examined in polished thin section using an Olympus BH2 polarizing microscope and a Nikon LABOPHOT2-POL polarizing and reflected light microscope. Freshly fractured rock fragments and polished thin sections were studied using a scanning electron microscope (SEM), a JEOL 5600 LV SEM at the University of Poitiers and a Hitachi S-3000 variable-pressure SEM at the Saskatchewan Research Council, both equipped with energy-dispersion spectrometers (EDS) for chemical analysis. SEM observations were made in secondary electron mode for morphological investigations on gold-coated slabs and in back-scattered electron mode for identification of APS on the basis of chemical contrasts in carbon-coated (JEOL SEM) and uncoated (Hitachi SEM) polished thin sections. The conditions of observation were as follows: beam current of 0.6 nA and accelerating voltage of 15 kV.

Electron microprobe analyses were obtained with a CAMECA SX 50 (University of Paris) and a JEOL JXA8600 Superprobe (University of Saskatchewan) using wavelength-dispersion spectrometery (WDS). Analytical data for Al, Sr, P, Ca, Ba, La, Ce, Nd, Pr, Fe, S, Th, and U were obtained (Table 2). The microprobes were calibrated using the following synthetic and natural standards: $SrSiO_3$, apatite, monazite, pyrite, NdCu, glass doped in rare earth elements, UO_2. Matrix corrections were made using a ZAF program. The analytical conditions were as follows: beam current of 20 nA; accelerating voltage of 15 kV; spot size of 2–4 μm; counting time of 30 to 40 s per element. The relative error on the elements sought is below 1.5%. The structural formulae of the APS minerals were calculated using a 6-cation normalization basis, as in the general APS mineral formula $AB_3(XO_4)_2(OH)_6$.

Whole-rock analyses were performed on half-core sections, each about 30 cm long, by ICP-MS analyses at the SARM laboratory (CRPG-CNRS, Nancy, France) (Table 3). Information on analytical conditions such as detection limits, accuracy, and precision is available at http://www.crpg.cnrs-nancy.fr/SARM/index.html.

Results

APS crystals are commonly rhombohedral and have a pseudocubic habit (Fig. 2a), and are closely associated with the clay matrix throughout the sandstone and clay-altered material in the basement lithologies. In the manner described by Rasmussen (1996), the APS minerals occur in the sandstone as clusters of minute euhedral crystals (Fig. 2b), 1–20 μm in size, within pockets of clay matrix, lining detrital quartz surfaces, and within early diagenetic quartz

TABLE 1. Petrologic observations on the APS-bearing samples from the Athabasca Basin

Samples	Location	Identified non APS minerals	Host rocks
1–2	Shea Creek (Anne deposit) and McArthur deposits	Sudoite, illite ± trioctahedral chlorite, monazite, pyrite, apatite	Altered metamorphic rocks, below the unconformity and altered sandstones close the unconformity
3–4	Cigar Lake and McArthur deposits	Sudoite, illite	Altered sanstones above unconformity
5–6	Anomalous prospects	Illite, sudoite ± trioctahedral chlorite, monazite, apatite, pyrite	Altered metamorphic rocks, close to the unconformity and discontinuities
7–8		Illite, sudoite	Altered sandstone above and close to the unconformity
9	Regional background	Trioctahedral chlorite	Unaltered basement rocks below the unconformity
10–11		Illite, hematite	Unaltered Athabasca sandstone, above the unconformity

TABLE 2. Electron microprobe analyses and structural formulae of APS minerals from the Athabasca Basin, Canada

Sample		Proximal alteration areas				Intermediate alteration areas				Distal alteration areas			
		1		3		5		7		9		11	
		Mean*	Std dv.	Mean*	Std dv.	Mean*	Std dv.	Mean*	Std dv.	Mean*	Std dv.	Mean*	Std dv.
	SrO	2.12	0.23	5.28	0.56	6.49	0.47	9.44	0.96	9.85	1.43	16.32	0.96
	CaO	1.25	0.36	3.17	0.57	2.47	0.26	2.50	0.22	3.69	0.37	3.14	0.61
	La_2O_3	6.11	0.28	4.68	1.00	4.51	0.40	3.27	0.28	2.15	0.73	0.15	0.19
	Ce_2O_3	12.19	0.24	8.05	0.80	7.08	0.33	5.69	0.40	3.43	0.78	0.39	0.35
	Pr_2O_3	1.33	0.15	0.84	0.21	0.64	0.10	0.74	0.13	0.33	0.15	0.07	0.07
	Nd_2O_3	3.72	0.55	2.44	0.62	1.95	0.26	1.45	0.15	1.10	0.22	0.11	0.10
	$Th0_2$	0.36	0.15	1.36	0.73	0.19	0.11	1.29	0.50	1.42	0.54	0.03	0.03
	Al_2O_3	28.94	0.43	30.78	1.10	29.09	0.47	30.51	1.72	29.91	0.61	31.98	0.93
	Fe_2O_3	0.24	0.16	1.08	0.52	1.69	0.24	0.69	0.40	2.61	1.43	0.26	0.13
	P_2O_5	25.99	0.66	27.15	1.26	25.60	0.51	25.21	1.36	25.40	0.40	23.61	1.04
	SO_3	1.24	0.26	2.21	0.49	2.47	0.27	3.99	0.56	4.27	0.57	7.06	1.21
	Total	83.49		87.04		82.54		85.03		84.16		83.11	
		apfu*	Std dv.	apfu*	Std dv.	apfu*	Std dv.	apfu*	Std dv.	apfu*	Std dv.	apfu*	Std dv.
A	Sr	0.11	0.01	0.24	0.02	0.32	0.02	0.45	0.04	0.46	0.06	0.74	0.04
	Ca	0.12	0.03	0.26	0.04	0.22	0.02	0.22	0.02	0.32	0.03	0.26	0.05
	La	0.20	0.01	0.15	0.03	0.14	0.01	0.01	0.01	0.06	0.02	0.00	0.01
	Ce	0.39	0.01	0.25	0.02	0.22	0.01	0.10	0.01	0.10	0.02	0.01	0.01
	Pr	0.04	0.00	0.03	0.01	0.02	0.00	0.17	0.00	0.01	0.00	0.00	0.00
	Nd	0.12	0.02	0.07	0.02	0.06	0.01	0.02	0.00	0.03	0.01	0.00	0.00
	ΣLREE	0.75	–	0.50	–	0.44	–	0.30	–	0.20	–	0.01	–
	Th	0.01	0.00	0.02	0.01	0.00	0.00	0.02	0.01	0.03	0.01	0.00	0.00
B	Al	2.99	0.03	2.94	0.04	2.90	0.02	2.94	0.02	2.84	0.09	2.97	0.03
	Fe	0.02	0.01	0.06	0.03	0.11	0.01	0.04	0.03	0.16	0.08	0.02	0.01
X	P	1.93	0.03	1.85	0.03	1.84	0.02	1.74	0.04	1.73	0.02	1.57	0.07
	S	0.08	0.02	0.15	0.03	0.16	0.02	0.24	0.03	0.26	0.03	0.42	0.06

Notes: U_2O_3 < *D.L.* Structural formulas were calculated on the basis of 6 cations per formula unit. Sample locations 1, 3, 5, 7, 9, 11 are given in Table 1.
* Mean analytical values are based on 10 microprobe analyses per sample.

overgrowth material. They occur less commonly in the sandstone with altered mica (Fig. 2c) or as thin rims lining cavities left following quartz grain removal. Rare crystals composed dominantly of the LREE-bearing APS end-member, locally form within detrital quartz grains along the surfaces of monazite inclusions (Fig. 2d). In the basement rocks and in the sandstone within a few meters above the unconformity, APS minerals are observed associated with clay alteration commonly encountered at the base of the basin, below the unconformity, and along the fault zones (Fig. 2e). Close to the unconformity, APS minerals also locally appear as clusters of minute crystals or as larger individual euhedral grains up to 50 µm in the paleoweathered basement (Fig. 2f) and become rarer with depth. APS minerals are best observed with SEM under BSE mode, due to their high relative atomic weight. They have a pseudocubic crystal habit in thin section that is unique in the sandstone. Some crystals, particularly in the basement, display a compositional zonation on a scale of less than 2 µm (Fig. 3a), which probably reflects changing elemental activities in the fluid during mineral precipitation (Rasmussen 1996).

Relationships between APS minerals and clay alteration

The APS minerals are commonly present as disseminated minerals associated with host-rock clay alteration around the Athabasca unconformity-type uranium deposits, as also demonstrated by Gaboreau et al. (2005) for the uranium deposits associated with the Kombolgie Formation of Australia. In both regions, the distribution and the nature of clay minerals are related to their position relative to the ore deposits and to the distance from the intensive fluid-rock interaction, which took place at the sub-Kombolgie unconformity. But in the Athabasca Basin, additional associations have also been distinguished.

In the Athabasca basin, diagenetic illite and kaolin are the most abundant clay minerals and are observed in pores between grains (Hoeve and Quirt 1984; Quirt 2001, 2003, among others). In a thin, decimeter-scale zone at the bottom of the basal Manitou Falls Formation, illite is commonly associated with variable amounts of di,trioctahedral chlorite (sudoite) and occasionally alkali-poor tourmaline (dravite), and forms a weak halo of diagenetic-hydrothermal alteration mostly on the sandstone side of the unconformity. Near unconformity-type uranium deposits and in barren host-rock alteration halos, illite and sudoite occur in hydrothermally altered sandstone and metasedimentary rocks of the basement near the unconformity, and in fault zones that intersect the unconformity (Hoeve and Quirt 1984; Quirt 1986; Wilson and Kyser 1987; Kotzer and Kyser 1995; Quirt 2003). Diagenetic-hydrothermal alteration illite has also been identified

TABLE 3. Representative whole-rock geochemical analyses (major and trace elements) APS-bearing samples

Drill hole	Depth (m)	Major elements (%)			Trace elements (ppm)						
		Fe_2O_3	Al_2O_3	P_2O_5	Sr	Th	U	La	Ce	Pr	Nd
Erica 1	50.7	0.00	0.30	0.00	75.37	1.88	0.39	12.83	27.19	12.83	11.68
Erica 1	113.3	0.20	0.58	0.00	44.62	1.99	0.44	8.09	18.02	8.09	7.18
Erica 1	162.6	0.17	0.41	0.06	84.22	1.88	0.49	8.63	18.17	8.63	7.30
Erica 1	232.1	1.50	0.44	0.18	919.52	2.10	0.58	7.86	15.34	7.86	6.17
Erica 1	303.2	1.92	0.41	0.07	132.52	2.80	0.68	12.65	27.94	12.65	9.35
Erica 1	359.0	0.18	0.90	0.00	71.24	3.17	0.39	10.57	21.60	10.57	7.17
Erica 1	417.2	0.17	0.61	0.00	91.76	2.51	0.42	10.72	24.16	10.72	8.98
Erica 1	454.2	7.48	2.03	0.00	175.32	8.00	1.20	15.10	34.25	15.10	14.65
Erica 1	511.4	0.25	0.96	0.06	64.41	3.27	0.86	8.73	19.60	8.73	7.66
Erica 1	598.5	0.30	2.21	0.05	122.17	6.15	0.65	11.03	25.65	11.03	10.25
Erica 1	652.7	0.00	0.48	0.00	54.52	1.80	0.84	5.14	11.26	5.14	4.52
Erica 1	710.2	0.56	0.73	0.00	50.13	3.81	0.77	11.77	25.27	11.77	9.61
Erica 2	55.0	0.00	0.36	0.00	94.24	2.33	0.38	15.08	33.84	3.49	12.40
Erica 2	102.2	0.10	1.25	0.00	52.33	2.52	0.42	11.16	24.68	2.79	9.53
Erica 2	159.5	0.11	0.30	0.00	34.00	1.96	0.43	8.63	19.12	1.93	6.33
Erica 2	213.5	2.94	0.49	0.00	109.25	3.06	0.54	13.10	26.98	2.80	9.01
Erica 2	281.6	0.78	0.42	0.00	76.82	3.63	0.62	13.42	28.91	2.81	9.93
Erica 2	364.6	0.74	0.31	0.05	75.40	3.05	0.57	12.15	27.84	2.72	9.20
Erica 2	420.6	1.06	0.58	0.05	77.43	4.01	0.73	13.75	31.37	3.22	10.74
Erica 2	497.1	0.15	0.41	0.00	46.22	1.88	0.43	9.54	20.57	2.05	7.21
Erica 2	568.4	0.11	0.36	0.00	24.75	1.51	0.50	5.95	14.06	1.37	4.58
Erica 2	630.2	0.13	0.71	0.05	29.99	1.35	0.46	5.96	14.87	1.42	5.75
Erica 2	681.5	0.10	0.42	0.00	12.42	1.60	0.51	4.64	9.63	1.00	3.50
Erica 2	729.7	1.29	2.12	0.00	69.52	5.95	0.76	13.47	29.51	2.77	10.06
Erica 3	37.2	0.35	0.60	0.06	119.19	2.82	0.46	18.97	40.20	4.46	16.28
Erica 3	88.1	0.13	0.54	0.05	83.80	2.96	0.42	14.70	31.90	3.32	12.06
Erica 3	152.0	0.00	0.46	0.00	44.98	2.60	0.54	9.44	18.83	2.01	6.62
Erica 3	218.4	2.06	0.47	0.00	48.18	2.40	0.58	10.70	21.72	2.25	7.83
Erica 3	261.7	1.13	0.34	0.00	60.76	3.47	0.77	11.91	28.25	2.80	10.07
Erica 3	330.8	0.71	0.72	0.00	108.04	3.90	0.79	13.80	30.26	3.03	10.72
Erica 3	406.8	0.22	0.80	0.00	88.15	3.89	0.76	13.39	28.82	2.78	10.02
Erica 3	509	0.00	0.44	0.00	64.92	2.28	0.88	11.31	22.78	2.19	7.87
Erica 3	595.7	0.74	1.10	0.05	60.74	5.60	0.75	7.88	17.57	1.79	6.43
Erica 3	613.4	0.19	2.08	0.00	42.27	3.03	0.75	7.33	16.00	1.73	6.10
Erica 3	639.7	0.00	0.58	0.00	20.28	2.31	0.82	6.26	13.02	1.38	4.75
Erica 3	695.1	0.00	0.82	0.05	35.10	4.18	0.99	11.00	22.84	2.56	9.73
She 77	34.7	0.14	0.63	0.05	91.02	2.60	0.80	15.25	32.73	3.58	13.14
She 77	86.7	0.00	0.43	0.00	41.26	2.39	0.58	8.68	18.09	1.86	6.36
She 77	153.7	0.11	0.45	0.00	43.56	3.03	0.57	8.61	17.90	1.78	5.49
She 77	193.2	0.45	0.39	0.00	63.89	3.22	0.59	9.55	19.88	1.96	6.79
She 77	275.1	0.61	0.45	0.00	194.35	5.24	1.15	12.19	28.66	2.96	10.12
She 77	352.3	0.15	0.53	0.05	92.12	3.45	0.84	11.46	25.54	2.53	9.01
She 77	447.1	0.16	0.48	0.00	44.11	2.51	0.90	7.70	16.79	1.69	5.80
She 77	516.7	0.27	1.04	0.00	58.96	3.58	0.70	9.03	19.66	1.89	6.57
She 77	604.5	0.26	0.84	0.00	37.20	3.04	0.98	6.23	12.39	1.25	4.59
She 77	648.8	1.60	0.54	0.00	80.79	6.11	2.14	8.04	17.58	1.90	6.99
She 77	687.8	0.00	2.01	0.00	61.81	3.43	0.82	10.56	22.56	2.34	8.47
She 77	728.5	0.00	0.25	0.00	13.19	3.37	4.67	5.24	9.98	1.00	3.40

in relatively distal drill holes, as well as in proximal and mineralized drill holes (Laverret et al. 2005). The presence of illite has resulted from several (re)crystallization processes that operated during diagenesis and/or the syn-ore alteration event.

Sudoite and dravite also occur locally in fault zones up to 700 m above the basal unconformity (e.g., the Colette deposit at Shea Creek), suggesting that these faults gave fluids that had interacted and equilibrated with basement lithologies access to much higher stratigraphic levels (Kister et al. 2006). Hydrothermal Mg-rich trioctahedral chlorite occurs in zones of strong alteration in Mg-rich metasediments and in the core of the diagenetic-hydrothermal alteration halos (Hoeve and Quirt 1984; Quirt 1986, 2003; Kotzer and Kyser 1995), and retrograde metamorphic Fe-Mg trioctahedral chlorite is found deeper in fresher basement rocks.

In barren sandstone, away from the unconformity, APS minerals are associated with diagenetic illite in pores between quartz grains. They are also found with retrograde metamorphic Fe-Mg trioctahedral chlorite deeper in the basement rocks (e.g., Quirt 1997a). In the weakly altered zone at the base of the sandstone and in the upper part of the regolith below the unconformity, they are associated with a finely mixed clay mineral assemblage composed of illite and sudoite with some relict kaolin. This association is also noted in the sandstone up to few hundred meters above the unconformity along faults. In the diagenetic-hydrothermal clay mineral alteration halos in the sandstone above the unconformity near the mineralized zones (e.g., Cigar Lake, McArthur River, Yalowega Lake), APS minerals are associated with massive clay mineral host-rock alteration composed of illite and sudoite, and more rarely Mg-rich trioctahedral chlorite in the core of the alteration halos. In mineralized zones in the basement, APS minerals are associated with illite, trioctahedral chlorite, and sudoite (e.g., McArthur River, Shea Creek).

Thus, three main associations of clay minerals and APS

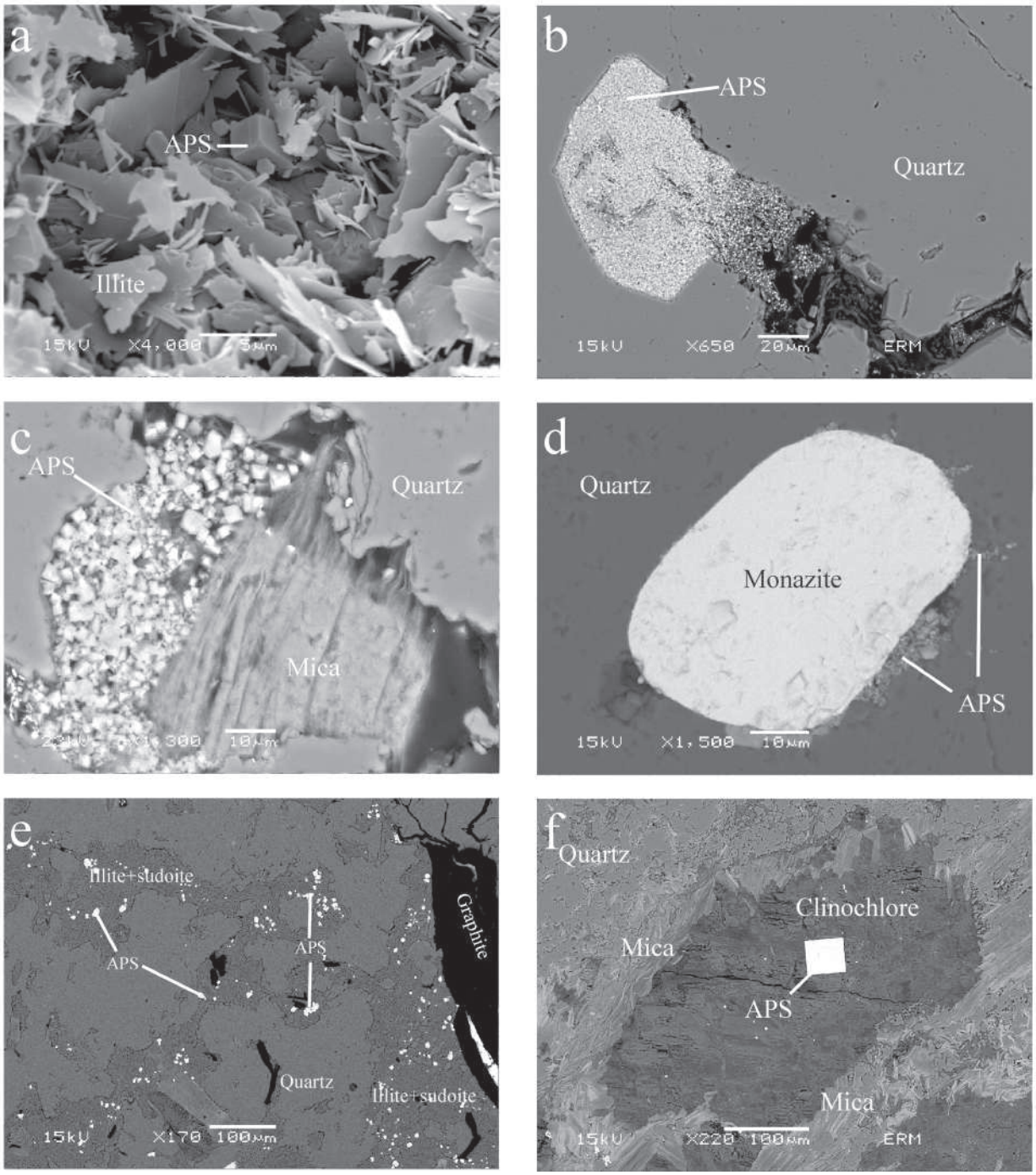

FIGURE 2. SEM images of APS minerals from the Athabasca Basin. (**a**) Pseudocubic habit of APS grain in illite matrix, from a distal alteration area. Length of scale bar is 5 µm. (**b**) Aggregate of small euhedral grains of APS minerals in sandstone intergranular pore space. (**c**) Cluster of APS minerals lining the surface of altered micas. (**d**) LREE end-member APS crystals along the surface of detrital monazite grain. (**e**) Disseminated crystals of LREE rich APS (white spots) in a matrix of hydrothermal illite + sudoite, from close to a discontinuity. (**f**) Larger euhedral APS crystal, from paleoweathered basement.

minerals can be considered:

(1) Kaolin + illite ± (hematite, APS minerals) in unaltered sandstone away from the unconformity and any mineralization.

(2) Illite + sudoite + hematite + APS minerals ± (dravite, pyrite, kaolin) in the different zones of weak clay alteration associated with faults and present adjacent to both sides of the unconformity away from zones of anomalous mineralization.

(3) Illite + sudoite + APS minerals + dravite ± (trioctahedral

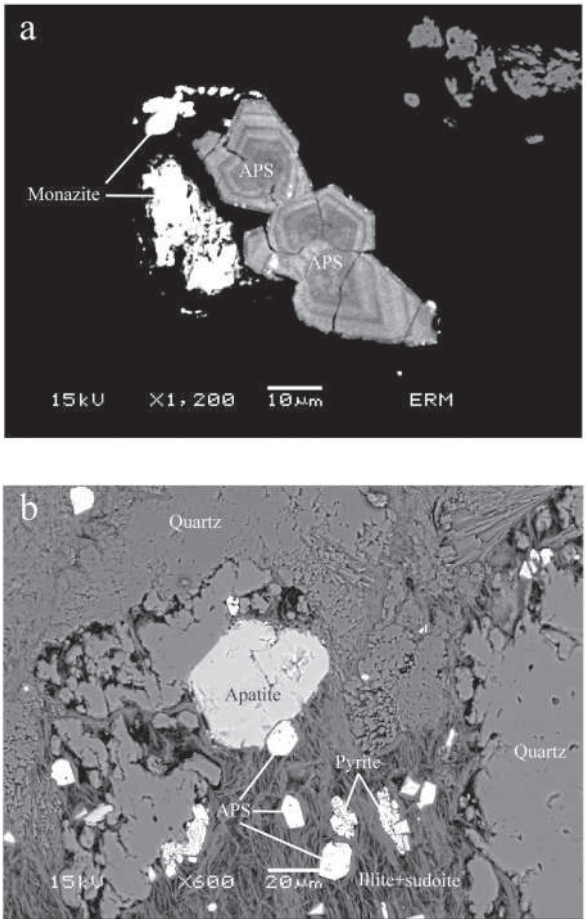

FIGURE 3. APS minerals in basement rocks. (**a**) Associated with relict monazite. (**b**) In contact with pyrite and apatite.

chlorite, hematite, pyrite, apatite) in the different zones of strong clay alteration associated with the mineralization process on both sides of the unconformity.

Relationships between APS minerals and other accessory minerals

The dominant potential source of aluminum for the precipitation of APS minerals in the Athabasca region is the intergranular clay mineral matrix (e.g., Gaboreau et al. 2005; Pe-Piper and Dolansky 2005). Similarly, detrital monazite and apatite are the dominant potential sources of REE, Ca, Sr, and P for the APS minerals (e.g., Fayek and Kyser 1997; Hecht and Cuney 2000), whereas pyrite is the dominant potential source for S (Quirt 2001). Close associations of these accessory minerals have been observed in the different samples used in this study, throughout the sandstone and the basement rocks.

In the sandstone, monazite is locally present within, and armored by, detrital quartz. In this location, further sites of mineral growth, as clusters of minute euhedral APS crystals on monazite grains, have been occasionally observed (Fig. 2d). In the basement rocks, alteration of monazite grains is apparent throughout the basement lithologies (Hecht and Cuney 2000). Associated with the ghosts of monazite grains, APS minerals sometimes display compositional zoning with alternation of light elements (dark zones by SEM) and heavy elements (bright zones by SEM), which have been described as alternating Ca-Sr-rich and LREE-rich zones (Gaboreau et al. 2005). APS minerals associated with these monazite alteration sites also show some inclusions of monazite (Fig. 3a). In basement rocks where apatite still persists, APS minerals are often observed to be in contact with subhedral grains of apatite (Fig. 3b). Stoffregen and Alpers (1987) have demonstrated a relationship between apatite and the precipitation of APS minerals. Contacts between pyrite and APS minerals are also often observed in the basement rocks (Fig. 3b), where a high-sulfidation environment and lowering of pH values favorable for the formation of APS minerals resulted from alteration of pyrite.

APS Chemistry

The general formula for the APS minerals is ideally $AB_3(XO_4)_2(OH)_6$, in which *A*, *B*, and *X* represent three different crystallographic sites: 12-fold-coordinated *A* sites, occupied by monovalent (H_3O, K, Na, Rb, NH_4, Ag, Tl, etc.), divalent (Ca, Sr, Ba, Pb, etc.), trivalent (Bi, REE) and, more rarely, tetravalent (Th) cations; sixfold-coordinated *B* sites, commonly occupied by $Al^{3+}$and Fe^{3+}; and fourfold-coordinated *X* sites, commonly occupied by S^{6+}, P^{5+}, and As^{5+}.

Representative results of electron microprobe analyses of APS minerals from the three types of alteration areas distinguished above are presented in Table 2. The chemical elements were selected for analysis on the basis of preliminary qualitative EDS investigations. The relatively low analytical totals (between 80 and 85 wt%) obtained in most of the analyses are due to the presence of hydroxyl ions in their mineral structure (up to 15%; e.g., crandallite) and to the small sizes of many of the analyzed APS grains, which are commonly smaller than the volume of sample emitting the secondary X-ray radiation. Consequently there may be a partial integration of the surrounding minerals and micropores in the volume analyzed by the electron beam. A deficiency of cations in the X-sites, either due to the presence of carbon in the crystal structure (undetectable by microprobe) or to a lack of X-site cations resulting from radiation damage induced by Th (Mordberg 2004), may also contribute to the low analytical totals. It should be noted that most of the chemical zonations observed by SEM in some APS crystals are too narrow to be analyzed individually with an electron microprobe and that the uranium content in all of the analyzed APS minerals was below detection limit.

For a better comparison of the APS compositional variations, APS mineral formulae were calculated from the results of the microprobe analyses on the basis of 6 cations per formula unit (Table 2). The analytical results fit the general formula for APS minerals and the data indicate the presence of complex chemical cation substitutions that form solid solutions among different compositional end-members: Sr^{2+}, $LREE^{3+}$, Ca^{2+}, Ba^{2+}, and Th^{4+} in the A-site; Al^{3+} and Fe^{3+} in the B-site; and P and S in the X-site. To balance charge formulae for APS minerals resulting from $(Sr, Ca)^{2+}$ substitution of $LREE^{3+}$, we have substituted $[PO_3OH]^{2-}$ for $[PO_4^{3-}]$, that is, negative charge is apportioned between O^{2-} and $(OH)^-$ to give a more general formula $AB_3[PO_3O_y(OH)_{1-y}]_x(SO_4)_{2-x}(OH)_6$.

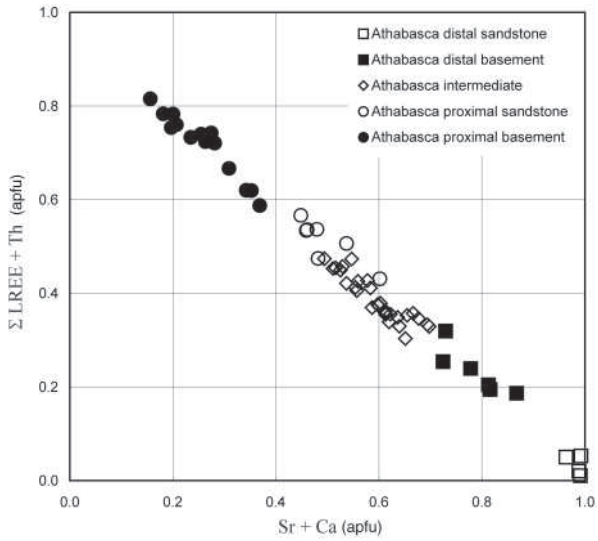

FIGURE 4. Plot of LREE + Th vs. Sr + Ca showing the relationship between the trivalent and tetravalent cations and the divalent cations for APS minerals from the Athabasca Basin.

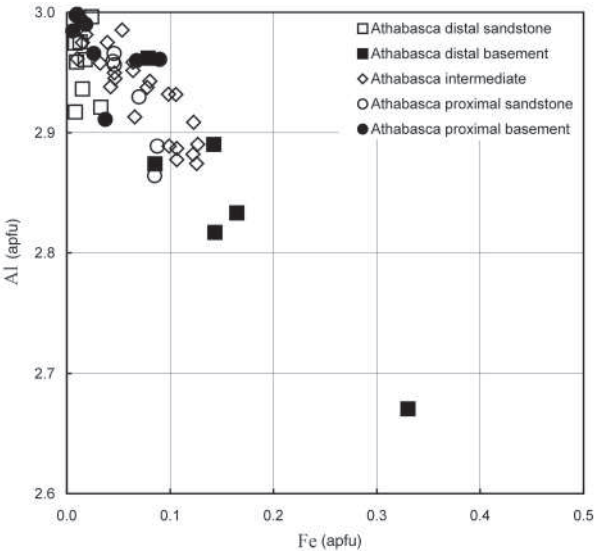

FIGURE 5. Plot of Al vs. Fe showing the B-site elemental relationship for APS minerals from the Athabasca Basin.

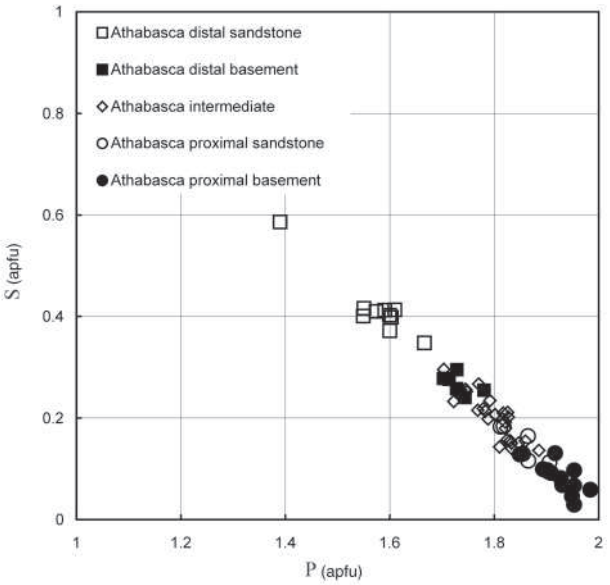

FIGURE 6. Plot of S vs. P showing the X-site elemental relationship for APS minerals from the Athabasca Basin.

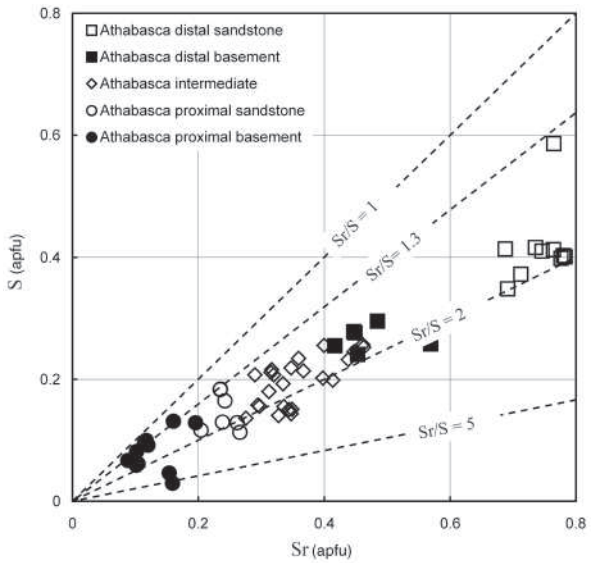

FIGURE 7. Plot of S vs. Sr showing the X- and A-site elemental relationships for APS minerals from the Athabasca Basin.

The inverse relationships between the A-site cations relate to the respective amounts of Sr + Ca and LREE (Fig. 4) or Th (in Th-rich APS). In the B site, there is a good inverse relationship between Fe and Al (Fig. 5), and, in concert with the A-site cation substitutions, P and S show an inverse relationship in the X site (Fig. 6). Sulfur and Sr are positively correlated with an average S/Sr ratio of ~1.9 (Fig. 7), although the ratio in the APS minerals found in the proximal basement alteration zone may vary from 1.3 to nearly 5.

The highest amounts of Sr and S, and the lowest amounts of LREE and P were found in APS minerals from the distal zones of alteration (Table 2). The APS observed in unaltered, barren sandstone far from the unconformity (Erica 1 in the western Athabasca; Rumple Lake in the middle of the basin) have compositions close to those of $\{SrAl_3[PO_3O_{0.5}(OH)_{0.5}]_2[OH]_6\}$, goyazite in current usage (Jambor 1999) and $[SrAl_3(PO_4)(SO_4)(OH)_6]$, an idealized svanbergite composition in current usage (Jambor 1999). Conversely, the lowest amounts of Sr and S and the highest amounts of LREE and P were found in APS minerals located close to the U deposits (Cigar Lake in the eastern Athabasca; Shea Creek in the western Athabasca), in particular in samples from the basement rocks, with compositions close to [LREE $Al_3(PO_4)_2(OH)_6$], florencite in current usage (Jambor 1999). APS minerals from the intermediate alteration zones located close to the principal discontinuities (unconformity, fractures, faults) present REE- and P-enriched chemical compositions intermedi-

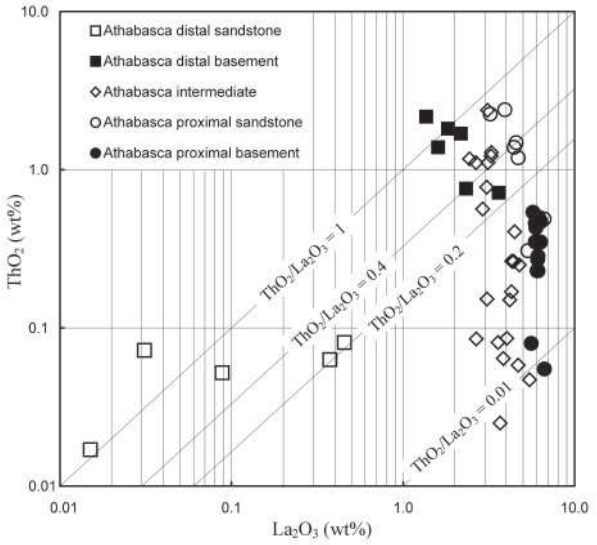

FIGURE 8. Plot of Th vs. La for APS minerals from the Athabasca Basin.

ate to, but distinct from, those of the other two zones of alteration. The APS minerals from all the alteration zones studied in the Athabasca Basin contain also small amounts of Ca, Th, and Fe. The Ca and Fe contents do not vary significantly throughout the different alteration zones. Thorium has a more heterogeneous distribution (Fig. 8), the lowest values being recorded in the APS from the distal alteration zones in the sandstone and the highest ones in the APS from the distal basement zones and a few from intermediate and proximal sandstone zones. The Th contents in the APS from intermediate and proximal sandstone are the most variable (0.04 to 2 wt%; Fig. 8).

Thorium enrichment is also responsible for local occurrences of increased radioactivity in conglomeratic sandstone of the lower Manitou Falls Formation (Mwenifumbo et al. 2002). The high Th content observed in these conglomeratic sandstones is due to the presence of very fine-grained Th-rich APS minerals in the intergranular pores; some of their compositions approach $[(Th,Pb)Al_3(PO_4)(SiO_4)(OH)_6]$, a possible composition for eylettersite (Jambor 1999). The Th-rich material occurs as rounded cores within the pseudocubic APS crystals, and is overgrown by Sr-rich APS similar to that found elsewhere in the Athabasca basin.

Whole-rock LREE and Th geochemistry

To evaluate the extension of the development of APS minerals and the associated REE transfer to the scale of the siliciclastic sequences in the Athabasca Basin, a systematic sampling and whole-rock major and trace element geochemical analysis program was carried out on sandstone from 4 drill hole cores distributed along an east-west profile in the western part of the basin (Erica-Shea Creek areas, 20 km south of the Carswell impact structure; Fig. 9), located away from the Shea Creek mineralization. Such a broad evaluation was not performed for the basement rocks because the exploration drill holes generally penetrate only a few tens of meters below the unconformity. Representative geochemical data are presented in Table 3.

Monazite represents the most abundant detrital Th- and LREE-hosting mineral in siliciclastic sediments (Overstreet 1967), but this mineral can be altered to various extents by diagenetic brines (Cuney and Mathieu 2000, and references therein). With Th being much less mobile than are the LREEs, the distribution of Th more accurately reflects the initial abundance of monazite in the sandstone. This relationship is supported in the Erica-Shea Creek section (Fig. 9) by the fact that the Th-rich layers in the sandstone correspond well to coarser grained beds, as shown by the plot of grain-size variation for the Erica 1 drill hole. Some coarse-grained layers in the upper part of the same drill hole do not contain high Th contents, because this part of the sedimentary sequence may have been derived from a relatively Th-poor source. In comparison, La (which is a proxy for the LREE as the other LREE show the same patterns) presents a completely different distribution along the same section (Fig. 9). The highest La contents do not coincide with the Th-rich layers and, on a regional basis, the La contents appear to be lower at the base of the sedimentary pile and it shows a relatively homogeneous distribution in stratigraphically higher levels. The difference between Th and La distributions suggests that the REE were mobile at the basin scale. The relative mobility of the REE is well demonstrated by the Th/La distribution along the Erica-Shea Creek section (Fig. 10) and on a Th vs. La binary diagram (Fig. 10). Clastic sediments worldwide present Th/La ratios between 0.2 and 0.4 (Cuney and Mathieu 2000 and references therein). Figure 10 clearly shows that many Athabasca samples present Th/La ratios higher than 0.4 suggesting LREE depletion, whereas others present Th/La ratios lower than 0.2, suggesting LREE accumulation relative to Th. In the Th/La section plot (Fig. 10), the layers containing the lowest LREE contents correspond to the ones which were the richest in Th and are interpreted to have been initially the richest in monazite, whereas the relatively LREE-enriched layers appear in the upper part of the section.

The differential mobility of the LREE and Th is also clearly indicated from the extremely variable Th/La ratios (from about 1 to less than 0.01) observed in the APS crystals (Fig. 10). Thorium being only weakly soluble, the amount of Th incorporated during formation of the APS minerals will depend on the proximity of the site of mineral crystallization to the source materials (i.e., the sites of altered monazite crystals). The Th/REE ratios of most APS minerals are not only higher than the average Th/La ratio of siliclastic metasediments, but also much higher than the Th/La ratios of the preserved monazite crystals from Athabasca sandstone and basement ($0.44 < Th/La < 1.07$), suggesting that the minerals crystallized far away from the altered monazite sites. Conversely, most APS crystals with relatively high Th/La ratios and high Th contents correspond to distal basement samples, which crystallized in the vicinity of altered monazite crystals, as indicated by their similar Th/La ratios.

DISCUSSION

Crystal chemical variations in APS minerals

Host-rock alteration petrography and the chemical data presented in this study demonstrate that APS minerals, coexisting with the different clay mineral parageneses in the Athabasca basin

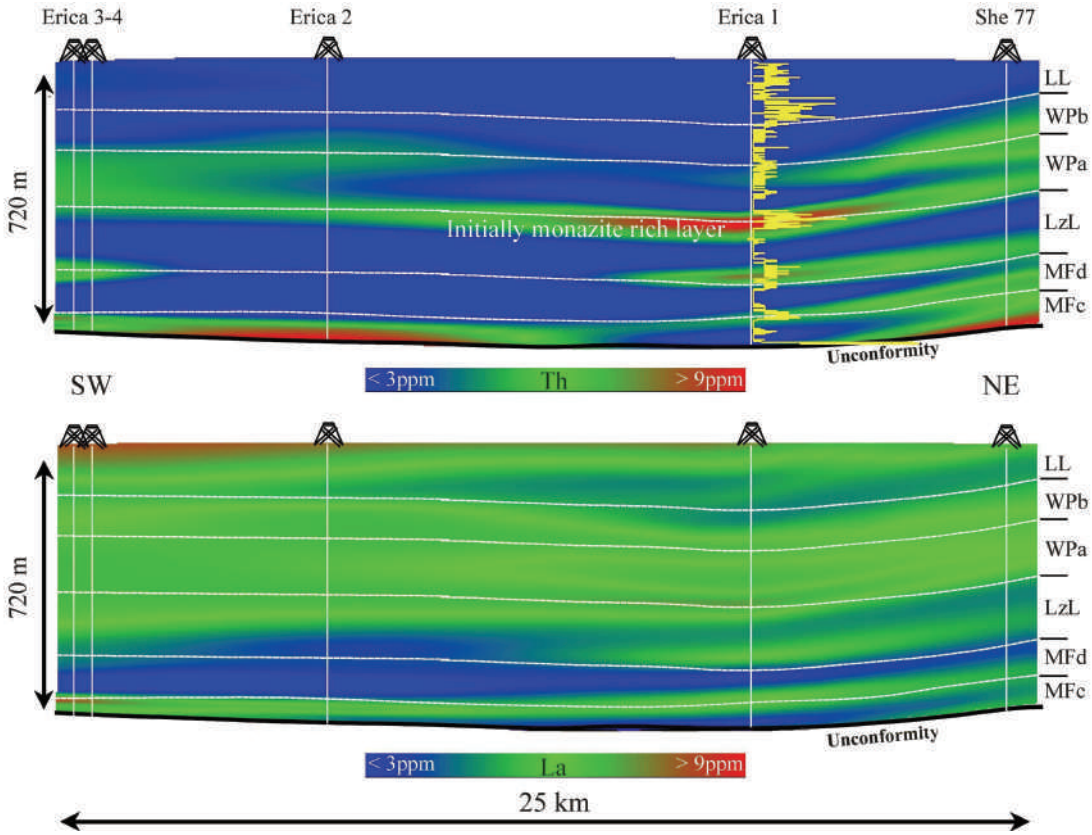

FIGURE 9. Th and La distributions from whole-rock geochemical analyses plotted along an east-west longitudinal profile in the western part of the Athabasca Basin. Maximum grain size in the sandstone is also plotted for drill hole Erica 1.

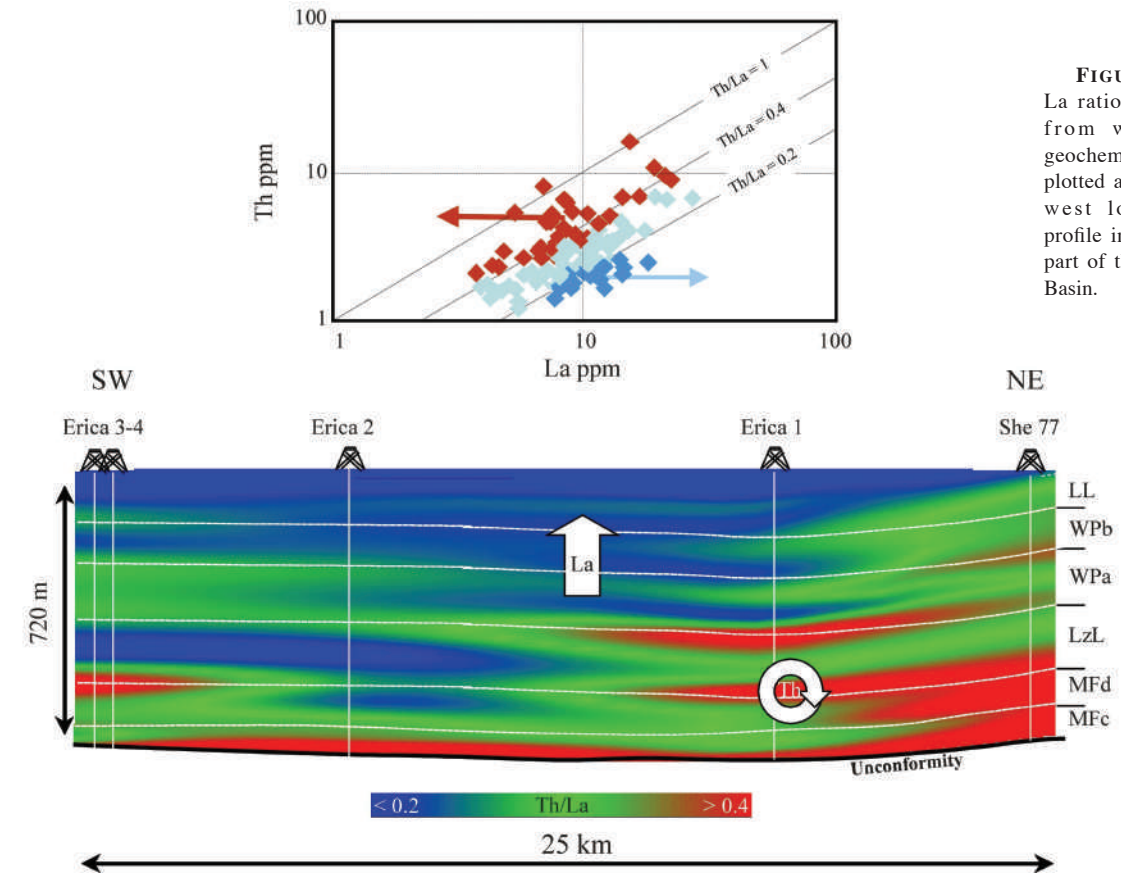

FIGURE 10. Th/La ratio distribution from whole rock geochemical analyses plotted along an east-west longitudinal profile in the western part of the Athabasca Basin.

and in the altered zones related to the Athabasca unconformity-type uranium deposits, exhibit wide ranges of chemical variation. These variations mostly consist of coupled substitutions of Sr + Ca for LREE and S for P in the A- and X-sites, respectively (Fig. 11), and Al and Fe in the B-site (Fig. 5).

According to the average compositions obtained for APS minerals from each alteration zone from both the sandstone and the metamorphic basement rocks (Table 2), representative crystal-chemical formulae have been calculated as follows:

(1) Distal alteration areas, unaltered (barren) areas:
Unaltered sandstone
$Sr_{0.74}Ca_{0.26}LREE_{0.01}(Al_{2.97}Fe_{0.02})[PO_3{\cdot}O_{0.65}(OH)_{0.35}]_{1.57}(SO_4)_{0.42}(OH)_6$;
Regolithic metamorphic basement rocks
$Sr_{0.46}Ca_{0.32}LREE_{0.20}Th_{0.03}(Al_{2.84}Fe_{0.16})[PO_3{\cdot}O_{0.77}(OH)_{0.23}]_{1.73}(SO_4)_{0.26}(OH)_6$.

(2) Intermediate alteration areas in basement rocks:
$Sr_{0.32}Ca_{0.22}LREE_{0.44}(Al_{2.90}Fe_{0.11})[PO_3{\cdot}O_{0.78}(OH)_{0.22}]_{1.84}(SO_4)_{0.16}(OH)_6$.

(3) Proximal alteration areas (U deposits):
U deposits hosted in sandstone
$Sr_{0.24}Ca_{0.26}LREE_{0.50}Th_{0.02}(Al_{2.94}Fe_{0.06})[PO_3{\cdot}O_{0.86}(OH)_{0.14}]_{1.85}(SO_4)_{0.15}(OH)_6$;

U deposits hosted in crystalline basement rocks
$Sr_{0.11}Ca_{0.12}LREE_{0.75}Th_{0.01}(Al_{2.99}Fe_{0.02})[PO_3{\cdot}O_{0.92}(OH)_{0.08}]_{1.93}(SO_4)_{0.08}(OH)_6$.

From the above listing, an increasing proportion of the REE in the APS solid solution coincides with (1) a decreasing distance from the uranium orebodies; (2) location in basement rocks; and (3) changes in the nature of the co-genetic clay mineral assemblages.

The overall compositional variation for the Athabasca APS minerals can be illustrated on a reciprocal diagram that shows the variations in S and P, and in Sr and LREE. It consists of a linear trend extending from the Sr and S-rich compositions of APS minerals from unaltered barren areas, through the altered sandstones of the distal alteration zone, to a LREE- and P-rich composition, that is close to florencite, for the APS minerals that are near to the uranium orebodies. However, the data collected in this study provide more details on the variations observed between these compositional poles. In particular, they show that, beyond the distance from the uranium orebodies and the changes in the nature of the co-genetic clay mineral assemblages, the chemical variations in APS minerals are also influenced by the host-rock lithology: for an equivalent alteration zone, the APS minerals formed in basement rocks are systematically enriched in P and LREE compared with those formed in sandstones (Fig. 12).

The variations in f_{O_2}-pH conditions between distal and proximal and basement zones are also in accordance with the chemical variations observed in the APS minerals. The f_{O_2}-pH conditions in the basin away from the mineralized zones are strongly oxidizing as attested by the ubiquitous hematite-rutile paragenesis with a slightly acidic pH controlled by the kaolinite-illite-quartz paragenesis (Hoeve and Quirt 1984; Kister et al. 2005). In the mineralized zones (with bleaching of the sandstones corresponding to hematite dissolution) and in the basement (containing graphite, sulfides, and Fe^{2+}-bearing silicates), more reduced conditions prevailed (Kister et al. 2006). The pH conditions were also somewhat more alkaline in the basement because of the common presence of K-feldspar with illite and quartz instead of kaolinite with illite and quartz in the sandstone (Kister et al. 2005). The relatively sulfate-rich APS minerals

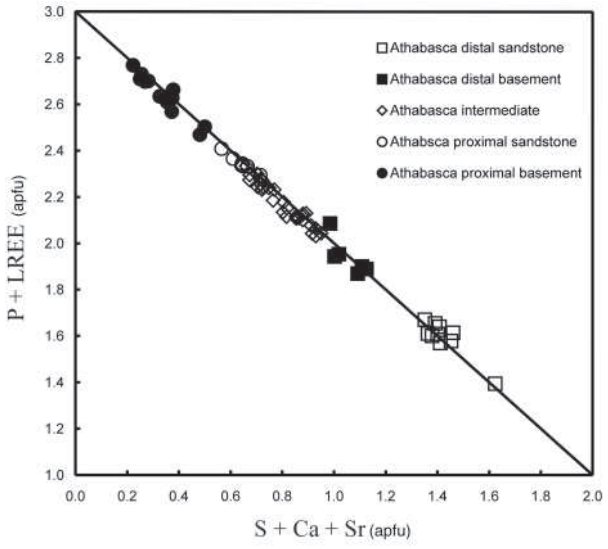

FIGURE 11. Plot of P + LREE vs. S + Ca + Sr showing the wide range of chemical compositions recorded in APS minerals from the Athabasca Basin.

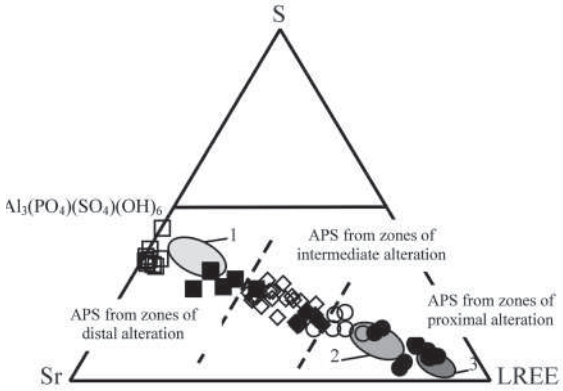

FIGURE 12. Reciprocal diagram based on Sr, S, and LREE electron microprobe analytical data for APS minerals from the Athabasca basin and the Kombolgie basin. Open symbols refer to APS compositions from sandstone and solid symbols refer to APS compositions from basement rocks. Fields 1, 2, and 3 refer to APS compositions from the Kombolgie Formation (Gaboreau et al. 2005): 1 = distal zones; 2 = intermediate alteration; 3 = zones of proximal alteration.

reflect the highly oxidizing conditions that prevailed in the distal sandstones, whereas in the reducing conditions that prevailed in the mineralized zones and in the basement, S occurred as a reduced species that cannot be incorporated the APS structure. Simultaneously, substitution of trivalent PO_4 by divalent SO_4 in the X-site allowed divalent cations (Sr, Ca) to enter the APS structure in the A-sites. Conversely, increasing trivalent LREE substitution in the A-sites requires increasing trivalent P content in the X-sites to maintain charge balance.

According to the modeling of APS stability by Komninou and Sverjensky (1996) and Gaboreau et al. (2005), Sr- and S-rich APS compositions are stable in the relatively acidic conditions with relatively high f_{O_2}, which are compatible with the composition of basinal fluids involved in the diagenetic reactions. Similarly, the LREE and P contents of APS minerals increase as conditions become more reducing and pH increases. The transition between LREE-rich APS and apatite that was observed at several scales (i.e., alteration sites of individual monazite and regional zoning in basement rocks) is also consistent with a higher neutralization of acidic diagenetic fluids by interaction with basement rocks. Indeed, APS minerals are more stable than apatite in lower pH environments in which LREE are mobile (Spötl 1990; Stoffregen and Alpers 1987; Vieillard et al. 1979).

Accordingly, the basement-hosted APS minerals and the APS minerals located in the vicinity of the U mineralization display high P/S ratios and high REE contents consistent with formation in more reducing conditions relative to the more distal APS minerals. The APS minerals from distal basement samples show low P/S consistent with oxidizing conditions during their formation, because they formed in an oxidized regolithic part of the basement (Macdonald 1980; Hoeve and Quirt 1984), which was not overprinted by the reducing conditions that developed in the vicinity of the mineralized zones. Therefore, the P/S ratio and the REE contents of the APS minerals can be considered to be markers of the relative variations of pH and oxygen fugacity in such environments (Fig. 13).

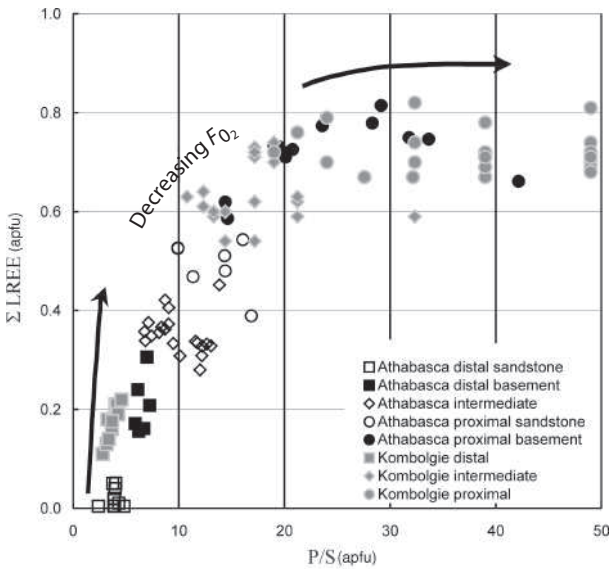

FIGURE 13. Plot of LREE vs. P/S ratio for APS minerals from the Kombolgie Formation (Gaboreau et al. 2005) and the Athabasca Basin. See text for discussion of the depicted f_{O_2} trend.

Source material for APS minerals

The above-noted variations in mineral chemical data give rise to the problem of the source material for the APS minerals encountered at different distances from the uranium orebodies in the unconformity-type deposits of both the Athabasca Basin and Australia.

The source material of the Sr-rich APS characteristic of the barren sandstones of the distal alteration areas is related to burial diagenesis in which this mineral represents the APS phase stable with the diagenetic basinal brines. Indeed, APS minerals with high Sr and S contents have been frequently reported in literature on sandstones worldwide (Rasmussen 1996; Spötl 1990; Dill 2001). The similar compositions of Sr-rich APS minerals from both the Athabasca Basin (this study) and the Kombolgie Formation (Gaboreau et al. 2005), in particular similar S/Sr ratios, and the commonly observed position of these crystals beneath and within early diagenetic quartz overgrowth material support the hypothesis of a similar diagenetic origin.

According to the chemical variations existing between the APS minerals of the alteration zones associated with the unconformity-type U of the East Alligator River Uranium Field, Gaboreau et al. (2005) suggested that the aqueous solutions, from which the Sr-rich APS in the distal sandstones were previously crystallized, were progressively richer in phosphorous and LREE with increasing proximity to the uranium ore deposits. Such concomitant enrichments in P and LREE toward the ore deposits suggest: (1) a common source of P and LREE elements, which consisted of dissolution of monazite in the basin and basement rocks, (2) an extensive mobility of P and LREE elements in the altered zones, and (3) decreasing f_{O_2}-pH conditions from distal sandstones to mineralized and basement zones. The parental links between basement monazite and APS minerals are supported by several items. (1) The first item is that of petrographic observations of neoformed APS at the alteration

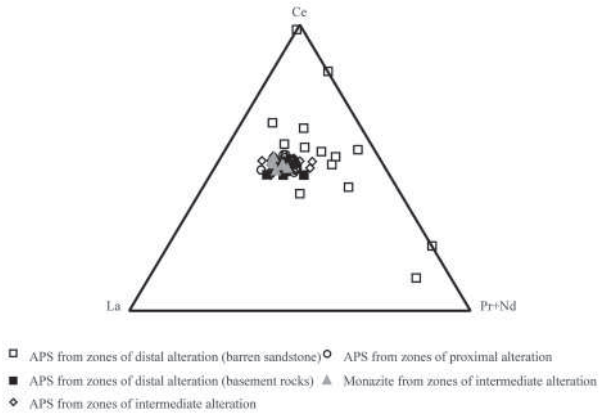

FIGURE 14. Ternary plot depicting La, Ce, and Pr + Nd electron microprobe analytical data for APS minerals and monazite from the Athabasca Basin.

sites of monazite within altered basement rocks and within the sandstone at locations where a fracture allowed the fluid to reach monazite crystals preserved in detrital quartz grains (Fig. 2d). (2) The second is the absence of LREE fractionation between the monazite crystals analyzed in the basement rocks and the APS minerals from both the sandstone and the basement rocks of the proximal and the intermediate alteration zones (Fig. 14). And (3) the third item is the systematic enrichment in the LREE end-member component of APS minerals in altered basement rocks in which primary monazite has been strongly to totally dissolved. However, Th, also a major component of monazite, does not follow the behavior of the LREE and presents an erratic distribution (Fig. 8), although the APS crystals growing far away from the altered monazite crystals are the poorest in Th because Th is much less mobile than the REE.

Because of the scarcity of preserved monazite crystals within the basin, a very limited amount of data show that LREE fractionation seems to exist between monazite and the APS of the distal sandstones (which contain less than 2% of the LREE end-member) with a strong depletion in La and a variable Ce/Pr+Nd ratio (Fig. 14). This trend may be related: (1) to a larger migration of the REE within the basin as observed in the Paleoproterozoic Francevillian sandstone (Cuney and Mathieu 2000), and (2) to a different origin which could be early diagenetic as already suggested by different authors (Hoeve and Quirt 1984; Wilson 1985; Quirt et al. 1991; Gaboreau et al. 2005). The source of S may have been sulfate derived from fluids expelled from possible overlying evaporitic formationsas suggested by the composition of the diagenetic brines and especially their extreme salinities and low Cl/Br ratios (Derome et al. 2005). However, the Douglas Formation shales and Carswell Formation dolomite are only preserved as a down-dropped rim around the Carswell impact structure in the western part of the Athabasca Basin and no evaporite sequences have been identified in the basin. The presence of trace amounts of preserved early diagenetic pyrite in the clastic formations (Quirt 2001) suggests that alteration/removal of much of the minor amounts of diagenetic pyrite originally present in the Athabasca sandstone is a likely source for the S now present in the APS minerals. The source of the phosphorus was likely from dissolution of detrital or diagenetic phosphates (Fayek and Kyser 1997) and monazite alteration.

The above considerations confirm that APS minerals are key minerals, which need to be investigated much more systematically in all types of environments and particularly in siliciclastic sedimentary basins.

Acknowledgments

The authors thank COGEMA (now AREVA) for financial support. Thierry Bonifait and Celine Boissard are thanked for their technical contributions. Critical reviews and comments by the two reviewers and associate editor are gratefully acknowledged

References cited

Andrade, N., Breton, G., Jefferson, C.W., Thomas, D., Tourigny, G., Wilson, S., and Yeo, G. (2002) Field Trip A1: The eastern Athabasca basin and its uranium deposits. Field trip guidebook, GAC-MAC joint annual meeting, Saskatoon, Saskatchewan, May 2002, 102 p.

Annesley, I.R., Madore, C., and Portella, P. (2005) Geology and thermotectonic evolution of the western margin of the Trans-Hudson Orogen: evidence from the eastern sub-Athabasca basement, Saskatchewan. Canadian Journal of Earth Sciences, 42, 573–597.

Beaufort, D., Patrier, P., Laverret, E., Bruneton, P., and Mondy, J. (2005) Clay alteration associated with Proterozoic unconformity-type deposits in the East Alligator Rivers Uranium Field, Northern Territory, Australia. Economic Geology, 100, 515–536.

Brouand, M., Cuney, M., and Deloule, E. (2003) Eastern extension of the Taltson orgenic belt and eastern provenance of Athabasca sandstone: IMS 1270 ion microprobe U/Pb dating of zircon from concealed basement plutonic rocks and from overlying sandstone (Canada). In M. Cuney, Ed., Uranium Geochemistry 2003, International Conference, April 13–16 2003, Proceedings: Unité Mixte de Recherche CNRS 7566 G2R, Université Henri Poincaré, Nancy, France, p. 91–94.

Card, C.D. (2001) Basement rocks in the western Athabasca basin in Saskatchewan. Summary of investigations 2001. Saskatchewan Geological Survey, Saskatchewan Energy and Mines, 321–333.

——— (2002) New investigations of basement to the western Athabasca basin. In Summary of Investigations 2002, Saskatchewan Geological Survey, Saskatchewan Energy and Mines, Miscellaneous Report 2002-4.2 CD-ROM, 17 p.

Card, C.D., Campbell, J.E., and Slimmon, W.L. (2003) Basement lithologic framework and structural features of the western Athabasca Basin. In Summary of Investigations 2003, Saskatchewan Geological Survey, Saskatchewan Industry and Resources, Miscellaneous Report 2003-4.2 CD-ROM, 17 p.

Card, C., Portella, P., Annesley, I., and Pana, D. (2006) Basement rocks to the Athabasca basin. In C.W. Jefferson and G. Delaney, Eds., EXTECH IV: Geology and Uranium Exploration Technology of the Proterozoic Athabasca basin. Saskatchewan and Alberta Saskatchewan Geological Society, Special Publication 17.

Cuney, M. (2005) World-class unconformity-related uranium deposits: key factors for their genesis. In J. Mao and F.P. Bierlein, Eds., Mineral deposits research: meeting the global challenge. Proceedings 8th Biennal SGA Meeting, Beijing, China, 3–7, 245–246.

Cuney, M. and Mathieu, R. (2000) Extreme light rare earth element mobilization by diagenetic fluids in the geological environment of the Oklo natural reactor zones, Franceville basin, Gabon. Geology, 28, 743–746.

Derome, D., Cuney, M., Cathelineau, M., Fabre, C., and Lhomme, T. (2002) Reconstitution of individual fluid inclusion composition using microthermometry, Raman microspectroscopy and Laser Induced Breakdown Spectroscopy. Application to the Shea Creek U deposit (Saskatchewan, Canada). GAC-MAC joint annual meeting, May 2002, Saskatoon, Saskatchewan, Abstracts, 27, 27.

Derome, D., Cathelineau, M., Cuney, M., Fabre, C., Lhomme, T., and Banks, D.A. (2005) Mixing of Sodic and Calcic Brines and Uranium Deposition at the McArthur River, Saskatchewan, Canada. A Raman and Laser-Induced Breakdown Spectroscopic Study of Fluid Inclusions. Implications on genetic models. Economic Geology, 100, 1529–1545.

Dill, H.G. (2001) The geology of aluminium phosphates and sulfates of the alunite group minerals: a review. Earth Science Reviews, 53, 35–93.

Ey, F., Piquard, J.P., Baudemont, D., and Zimmerman, J. (1991) The Sue uranium deposits, Saskatchewan, Canada; in new developments in uranium exploration, resources, production and demand. Proceeding in technical committee meeting jointly organized by the International Atomic Energy Agency and the Nuclear Agency of the OECD, Vienna, 189–213.

Fayek, M. and Kyser, T. (1997) Characterization of multiple fluid-flow events and rare-earth-element mobility associated with formation of unconformity-type uranium deposits in the Athabasca Basin, Saskatchewan. The Canadian Mineralogist, 35, 627–658.

Gaboreau, S., Vieillard, Ph., Patrier, P., Bruneton, P., and Beaufort, D. (2003) Aluminium phosphate sulfate minerals associated with unconformity uranium deposits of the Kombolgie basin (Northern Territory, Australia). In M. Cuney, Ed., Uranium Geochemistry, International Conference Proceedings Nancy, 157–160.

Gaboreau, S., Beaufort, D., Vieillard, Ph., Patrier, P., and Bruneton, P. (2005) Aluminum phosphate-sulphate minerals associated with Proterozoic unconformity-type uranium deposits in the East Alligator River Uranium Field, Northern Territories, Australia. Canadian Mineralogist, 43, 813–827.

Hecht, L. and Cuney, M. (2000) Hydrothermal alteration of monazite in the Precambrian crystalline basement of the Athabasca basin (Saskatchewan, Canada): implications for the formation of unconformity-related uranium deposits. Mineralium Deposita, 35, 791–795.

Hoeve, J. and Quirt, D. (1984) Mineralization and host rock alteration in relation to clay mineral diagenesis and evolution of the middle-Proterozoic Athabasca basin, northern Saskatchewan, Canada. Research Council Technical Report, 187, 187 p.

Hoeve, J. and Sibbald, T.I.I. (1978) On the genesis of Rabbit Lake and other unconformity-type uranium deposits in northern Saskatchewan, Canada. Economic Geology, 73, 1450–1473.

Jambor, J.L. (1999) Nomenclature of the alunite supergroup. Canadian Mineralogist, 37, 1323–1341.

Kister, Ph., Vieillard, Ph., Cuney, M., Quirt, D., and Laverret, E. (2005) Thermodynamic constraints on the mineralogical and fluid composition evolution in a clastic sedimentary basin: the Athabasca basin (Saskatchewan, Canada). European Journal of Mineralogy, 17, 325–342.

Kister, Ph., Laverret, E., Quirt, D., Cuney, M., Patrier, P., Beaufort, D., and Bruneton, P.

(2006) Mineralogy and geochemistry of the host-rock alterations associated to the Shea Creek unconformity-type uranium deposits (Saskatchewan, Canada), Part 2. Spatial distribution of the Athabasca Group sandstone matrix minerals. Clays and Clay Minerals, 54, 295–313.

Kolitsch, U. and Pring, A. (2001) Crystal chemistry of the crandallite, beudantite, and alunite groups: a review and evaluation of the suitability as storage materials for toxic metals. Journal of Mineralogy and Petrology Sciences, 96, 67–78.

Komninou, A. and Sverjensky, D.A. (1996) Geochemical modeling of the formation of an unconformity-type uranium deposit. Economic Geology, 91, 590–606.

Kotzer, T.G. and Kyser, T.K. (1995) Petrogenesis of the Proterozoic Athabasca basin, northern Saskatchewan, Canada, and its relation to diagenesis, hydrothermal uranium mineralization and paleohydrology. Chemical Geology, 120, 45–89.

Laverret, E., Patrier, P., Beaufort, D., Kister, Ph., Quirt, D., Bruneton, P., and Clauer, N. (2005) Mineralogy and geochemistry of host-rock alterations associated with the Shea Creek unconformity-type uranium deposits (Saskatchewan, Canada). Part 1: spatial variation of illite properties. Clays and Clay Minerals, 54, 275–294.

Lewry, J.F. and Sibbald, T.I.I. (1979) A review of pre-Athabasca basement geology in northern Saskatchewan. In G.R. Parslow, Ed., Uranium exploration techniques Regina, Saskatchewan, 1978, Symposium Proceedings, Saskatchewan Geological Society, Special Publication, 4, 91–99.

——— (1980) Thermotectonic evolution of the Churchill Province in northern Saskatchewan. Tectonophysics, 68, 45–82.

Lorilleux, G. (2001) Les brèches associées aux gisements d'uranium de type discordance du bassin d'Athabasca (Saskatchewan, Canada), 319 p. Unpublished Ph.D. thesis, Université Henri Poincaré, Nancy, France.

Lorilleux, G., Jebrak, M., Cuney, M., and Baudemont, D. (2002) Polyphase hydrothermal breccias associated with unconformity-type uranium mineralization (Canada): from fractal analysis to structural significance. Journal of Structural Geology, 24, 323–338.

Lorilleux, G., Cuney, M., Jebrak, M., Rippert, J.C., and Portella, Ph. (2003) Chemical brecciation processes in the Sue unconformity-type uranium deposits, eastern Athabasca basin (Canada). Journal of Geochemical Exploration, 80, 241–258.

Macdonald, C. (1980) Mineralogy and geochemistry of a Precambrian regolith in the Athabasca basin, 151 p. Unpublished M.Sc. thesis, University of Saskatchewan, Saskatoon.

——— (1985) Mineralogy and Geochemistry of the sub-Athabasca regolith near Wollaston Lake. In T.I.I. Sibbald and W. Petruk, Eds., Geology of uranium deposits. The Canadian Institute of Mining and Metallurgy, special volume 32, 155–158.

Marlatt, J., McGill, B., Matthews, R., Sopuck, V., and Pollock, G. (1992) The discovery of the McArthur uranium deposit, Saskatchewan, Canada. In New Developments in Uranium Exploration, Resources, I.A.E.A and the Nuclear Energy Agency of the Organization for Economic cooperation Development, Vienna, 26–29 August, 1991, IAEA-TECDOC, 650, 118–127.

McGill, B.D., Marlatt, J.L., Matthews, R.B., Sopuck, V.J., and Homeniuk, L.A. (1993) The P2 North uranium deposit, Saskatchewan, Canada. Exploration and Mining Geology, 2, 321–331.

Miller, A.R. (1983) A progress report: uranium phosphorus association in the Helikian Thelon Formation and sub-Thelon saprolite, central district of Keewatin. Geological Survey of Canada, 83-1A, 449–456.

Mordberg, L.E. (2004) Thorium in crandallite-group minerals: an example from a Devonian bauxite deposit, Timan, Russia. Russian Research Geological institute (VSEGEI), St. Petersburg, Russia. Mineralogical Magazine, 68(3), 489–497.

Mwenifumbo, C.J., Elliott, B.E., Drever, G., and Wood, G. (2002) Borehole geophysical logging of two deep surface boreholes and one underground borehole at McArthur River. In Summary of Investigations 2002, Saskatchewan Geological Survey, Saskatchewan Industry and Resources, Miscellaneous Report 2002-4.2, CD-ROM, Paper D-5, 5 p.

Overstreet, W.C. (1967) The geologic occurrence of monazite. United States Geological Survey, Professional Paper, 530, 327 p.

Pacquet, A. and Weber, F. (1993) Pétrographie et minéralogie des halos d'altération autour du gisement de Cigar Lake et leurs relations avec les minéralisations. Canadian Journal of Earth Sciences, 30, 674–688.

Pagel, M., Poty, B., and Sheppard, S.M.F. (1980) Contributions to some Saskatchewan uranium deposits mainly from fluid inclusion and isotopic data. In S. Ferguson and A. Goleby, Eds., Uranium in the Pine Creek Geosyncline, IAEA, Vienna, 639–654.

Pe-Piper, G. and Dolansky, L.M. (2005) Early diagenetic origin of Al phosphate-sulfate minerals (woodhouseite and crandallite-series) in terrestrial sandstones, Nova Scotia, Canada. American Mineralogist, 90, 1434–1441.

Percival, J.B., Bell, K., and Torrance, J.K. (1993) Clay mineralogy and isotope geochemistry of the alteration halo of the Cigar Lake uranium deposit. Canadian Journal of Earth Sciences, 30, 689–704.

Quirt, D.H. (1986) Host-rock alteration in the Spring Point area, northern Saskatchewan. Saskatchewan Research Council, publication number R-855-8-E-86.

——— (1997a) Chloritization below the Dawn Lake uranium deposit (11A Zone), northern Saskatchewan. GAC-MAC joint annual meeting, abstract volume 22, A-122.

——— (1997b) Geochemistry, host-rock alteration, mineralization, and uranium metallogenesis of the Wollaston Eagle project area. In Thermotectonic and uranium metallogenetic evolution of the Wollaston Eagle project area, Saskatchewan Research Council, publication number R-1240-2-C-97, 98 p.

——— (2001) Kaolinite and dickite in the Athabasca sandstone, Northern Saskatchewan, Canada. Saskatchewan Research Council, publication number 10400-16D01.

——— (2003) Athabasca unconformity-type uranium deposits: one deposit type with many variations. In M. Cuney, Ed., Uranium Geochemistry 2003, Nancy, International Conference Proceedings, 309–312.

Quirt, D., Kotzer, T., and Kyser, T.K. (1991) Tourmaline, phosphate minerals, zircon, and pitchblende in the Athabasca group: Maw zone and McArthur River Areas, Saskatchewan. In Summary of investigations 1991, Saskatchewan Geological Survey, miscellaneous report, 91(4), 181–191.

Rainbird, R., Stern, R.A., Rayner, N., and Jefferson, C.W. (2005) Age, provenance, and regional correlation of the Athabasca Group, Saskatchewan and Alberta constrained by igneous and detrital zircon geochronology. In C.W. Jefferson and G. Delaney, Eds., EXTECH IV: Geology and EXploration TECHnology of the Proterozoic Athabasca basin, Saskatchewan and Alberta. Geological Survey of Canada, bulletin 588.

Ramaekers, P. (1981) Hudsonian and Helikian basins of the Athabasca Region, Northern Saskatchewan. In F.H.A. Campbell, Ed., Proterozoic Basins of Canada Geological Survey of Canada, 81(10), 219–233.

——— (1990) Geology of the Athabasca Group (Helikian) in Northern Saskatchewan. Saskatchewan Energy and Mines, report 195, 49.

Ramaekers, P. and Catuneanu, O. (2004) Development and sequences of the Athabasca basin, Early Proterozoic, Saskatchewan and Alberta, Canada. In P.G. Eriksson, W. Altermann, D.R. Nelson, W.U. Mueller, and O. Catuneanu, Eds., The Precambrian Earth: Tempos and Events, Developments in Precambrian Geology, 12, p. 705–723. Elsevier Science Ltd., Amsterdam.

Ramaekers, P., Yeo, G., and Jefferson, C. (2001) Preliminary overview of regional stratigraphy in the late Paleoproterozoic Athabasca basin, Saskatchewan and Alberta. In Summary of Investigations 2001. Saskatchewan Geological Survey, miscellaneous report 2001-4.2 CD-ROM, 12 p.

Ramaekers, P., Jefferson, C.W., Yeo, G.M., Collier, B., Long, D.G., Catuneanu, O., Bernier, S., Kupsch, B., Post, R., Drever, G., McHardy, S., Jircka, D., Cutts, C., and Wheatley, K. (2005) Revised geological map and stratigraphy of the Athabasca Group, Saskatchewan and Alberta. In C.W. Jefferson and G. Delaney, Eds., EXTECH IV: Geology and Exploration Technology of the Proterozoic Athabasca basin, Saskatchewan and Alberta. Geological Survey of Canada, bulletin 588.

Rasmussen, B. (1996) Early-diagenetic REE-phosphate minerals (florencite, gorceixite, crandallite, and xenotime) in marine sandstones: a major sink for oceanic phosphorus. American Journal of Science, 296, 601–632.

Ruzicka, V. (1993) Unconformity-type uranium deposits. In R.V. Kirkham, W.D. Sinclair, R.I. Thorpe, and J.M. Duke, Eds., Mineral deposit modeling. Geological Association of Canada, special paper 40, 531–540.

Scott, K.M. (1987) Solid solution in, and classification of, gossan-derived members of the alunite-jarosite family, northwest Queensland, Australia. American Mineralogist, 72, 178–187.

Sibbald, T.I.I., Quirt, D.H., and Gracie, A.J. (1990) Uranium deposits of the Athabasca basin, Saskatchewan. In Field Trip 11 Guidebook, 8th IAGOD Symposium, Ottawa, Ontario. Geological Survey of Canada, open file 2166, 72 p.

Spötl, C. (1990) Authigenic aluminium phosphate-sulfates in sandstones of the Mitterberg Formation, northern calcareous Alps, Austria. Sedimentology, 37, 837–845.

Stoffregen, R.E. and Alpers, C. N. (1987) Woodhouseite and svanbergite in hydrothermal ore deposits: products of apatite destruction during advanced argillic alteration. Canadian Mineralogist, 25, 201–211.

Thomas, D.J., Matthews, R.B., and Sopuck, V. (2000) Athabasca Basin (Canada) unconformity-type uranium deposits: exploration model, current mine developments and exploration directions. In J.K. Cluer, J.G. Price, E.M. Struhsacker, R.F. Hardyman, and C.L. Morris, Eds., Geology and Ore Deposits 2000: The Great Basin and Beyond, Geological Society of Nevada Symposium Proceedings, May 15–18, 2000, CD-ROM, 103–125.

Thomas, D.J., Jefferson, C.W., Yeo, G.M., Card, C., and Sopuck, V.J. (2002) The Eastern Athabasca basin and its uranium deposits. Field trip guidebook, GAC-MAC, Saskatoon, Saskatchewan, May 2002.

Vieillard, Ph., Tardy, Y., and Nahon, D. (1979) Stability fields of clays and aluminium phosphates: parageneses in lateritic weathering of argillaceous phosphatic sediments. American Mineralogist, 64, 626–634.

Wilson, J.A. (1985) Crandallite group minerals in the Helikian Athabasca group in Alberta, Canada. Canadian Journal of Earth Sciences, 22, 637–641.

Wilson, M.R. and Kyser, T.K. (1987) Stable isotope geochemistry of alteration associated with the Key Lake uranium deposit. Economic Geology, 82, 1450–1557.

MANUSCRIPT RECEIVED APRIL 3, 2006
MANUSCRIPT ACCEPTED SEPTEMBER 17, 2006
MANUSCRIPT HANDLED BY EDWARD GREW